

Effect of soft-segment chemistry on polyurethane biocompatibility*

V. MELNIG*, A. GARLEA, L. OBREJA

Faculty of Physics, "Al. I. Cuza" University, Bd. Carol I, Nr. 11A, Iasi, 700506, Romania

Biodegradable synthetic polymers are widely used as biomaterials because their mechanical and physical properties that can readily be adjusted by varying the preparation techniques and controlling the primary, secondary and supra-molecular structure. In this paper, the effect of lactate soft-segment chemistry on biomimetic properties of polyurethane elastomer was studied by combining steady-state infrared spectroscopy and UV-ellipsometry scattering techniques, monitoring the orientation of different functional groups with a diaphragm type film specimen under static loading conditions - static linear dichroism (SLD). The SLD data were explained by hydrogen bonds rearranging process and competition orientations of different secondary structures segments during structural changes induced by stretching. The shape of secondary structure of studied polyurethanes depends on urethane group concentration and soft segment structure.

(Received October 5, 2005; accepted after revision May 18, 2006)

Keywords: Polyurethanes, Films, Steady-state linear dichroism, Stretching-secondary, Structure monitoring

1. Introduction

Biopolymers form complex architectures that are capable of sophisticated functions, due to special properties resulting from the characteristics of the complex sharply matched sequences of monomer units, amino acids or nucleotides, which are able to supra-structure and interact with the biological medium, since of the sophisticated biological assemble in specific sequences synthesis apparatus.

In contrast, polymers are simple structural materials with polydispersity, non-specific sequence and low polycrystallinity, but including an expanded alphabet of monomer units, enhanced stability and ability to form stable secondary structures, have some advantages over biopolymers [1].

While the natural polymer have complete biodegradability, poor strength due to water absorption and difficult prediction degradation kinetic rate, synthetic polymers have selected biodegradability that can be many times an advantage.

The most widely investigated and advanced biodegradable polymers in regard to available toxicological and clinical data are the aliphatic polyesters based on lactic and glycolic acids.

Despite of molecular instability and calcifications of polyurethanes that is a problem for long-lasting implants, it could be deliberately exploited to design biodegradable biomaterials by labile segments incorporation into the

polymer chain. By controlling hydrophilic/hydrophobic segment ratios, such biodegradable elastomers could be preferable for tissue adhesion barriers and/or adhesion and proliferation of various cell types [2].

Typically, a stable secondary structure is defined by stiffness of the monomer units, a conformational preference at the single bonds linking the units and alternant piling by aromatic interaction in helical structure longer than one helix tour. Similar secondary structure in polyurethane and polyurethane with lactate segment, with that of biopolymers, was obtained in casting prepared films. The present paper investigates the secondary and supra-molecular structure of linear polyester-urethanes, by SLD combined techniques.

2. Experimental

Synthesis of biocompatible poly(lactaturethane) (PL) and poly(esterurethane) (PU) precursor (Fig. 1) have been presented elsewhere [3, 4]. The average molecular weight number, determined by gel permeation chromatography, was 56,000 Da for PU and 58,000 Da for PL.

PL and PU films were prepared by dry phase inversion method [5], PL film being comparatively analysed with precursor PU film.

The morphology of film samples was studied by scanning electronic microscopy (SEM) on a TESLA-BS-300. The secondary and quaternary structures have been monitored by means of steady-state linear dichroism techniques, monitoring the orientation of different functional groups with a diaphragm type film specimen

* presented to 8th Romanian Biophysics Conference, May 26-28, 2005, Iasi, Romania

under static loading conditions (SLD). Static Linear Dichroism-Infrared (SLD-IR) was performed using a BOMEM MB-104 spectrometer with 4 cm^{-1} resolution in the range $4000\text{--}500\text{ cm}^{-1}$, and combined UV-ellipsometry

scattering techniques (SLD-UV) with a SLM 8000 spectrofluorometer, using 2 mm slit widths that involves a spectral bandwidth of 4 nm.

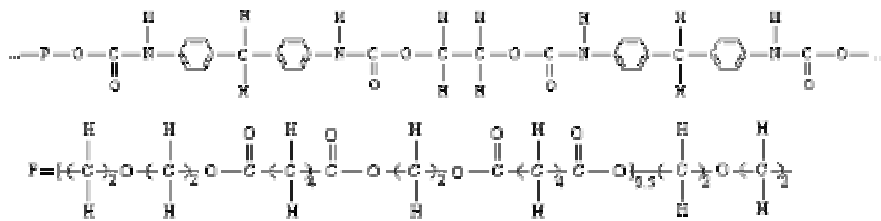


Fig. 1. Primary structure of polyurethane.

Infrared linear dichroism experiments supply molecular-level insight into the tensile properties of the polymer by monitoring the orientation of different functional groups [6]. In spectroscopic experiments the different domain behaviour can be monitored using well defined bands from correlation charts.

In the oriented samples, the directional properties associated with the transition dipole moments can be detected by recording polarized IR spectra along a particular direction. The dichroic ratio:

$$R = \frac{\Phi_{\text{ordinary}}}{\Phi_{\text{extraordinary}}}, \quad (1)$$

can be considered as an order degree indicator of molecular orientation and/or segmental mobility, in the polymer film and represents the ratio between integral absorption of parallel (Φ_{ordinary}) and perpendicular ($\Phi_{\text{extraordinary}}$) polarized radiation of a specific chemical group characteristic band.

The results indicate whether a particular bond is oriented parallel or perpendicular to the secondary fibre axis; by secondary structure in this work are named the α -helix and β -sheet ordered structures.

In order to obtain more information about symmetry (anisotropy) of the weak interactions involved in self-assembling of polymer, the second order Rayleigh scattering has used.

Rayleigh scattering represent the dispersion (elastic scattering) of electromagnetic radiation by particles that have a radius less than approximately $1/10$ the wavelength of the radiation. The first order Rayleigh scattering appears in spectrum at the some excitation wavelength and the second order at exactly double excitation wavelength. If the wavelength is set at the maximum molecule like fluorophore absorption band, the linear polarized light can be depolarized with a specific degree, that depend on the nature of the active fluorescent transition dipole moments. In the some style that in UV-VIS-IR ellipsometry [7] and Raman [8] techniques it defined the depolarization ratio:

$$\rho = \left(\frac{\Phi_{\text{ordinary}}}{\Phi_{\text{extraordinary}}} \right)^{-1}. \quad (2)$$

If the geometry of molecules is spherical and the symmetry of fluorophore dipole moments is high, the polarization of incident beam is maintained after scattering and the depolarization ratio is very small. In contrast, if the geometry of molecules is less in symmetry and/or transition fluorophore dipole moments distorts the symmetry of scattering potential, a significant depolarization can occur. For symmetric scattering potential, theory predict a depolarization ratio value $\rho < 0.75$, otherwise more that this value.

The set-up arrangement is similar to that used in refractive index ellipsometry measurements [7]. Film samples were placed in spectrofluorometer at the diagonal position of a cuvette chamber. This confers a 45° relative position of excitation monochromator polarizer and detector polarizer with normal of the film plane, and 90° between the two polarizers.

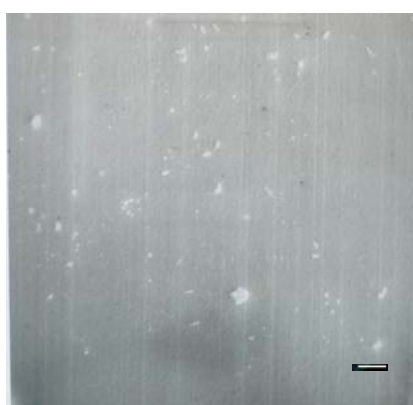
The spectra were obtained at room temperature in air, excitation beam was set at 395 nm maximum absorption band of UV-VIS spectrum; ordinary and extraordinary polarized states of second order Rayleigh scattering 790 nm maximum absorption bands of emission spectra have been recorded in two modes: axis of excitation linear polarized light form with normal weight lead thread 1) 0° and 2) 90° .

3. Results

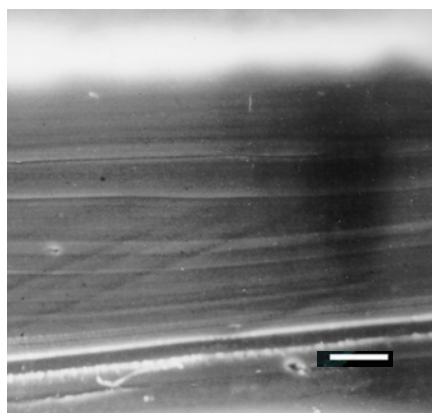
In Fig. 2 are presented SEM specimen photos of air facing of polyurethane films (PL (a) and PU (b)) and transversal section film of PU (c). The prepared films were thin, transparent, flexible, and compact (no pores – see Fig. 2c). The thickness of specimen films for SLD-IR was less than $50\ \mu\text{m}$ in order to perform good optical transparency.



(a)



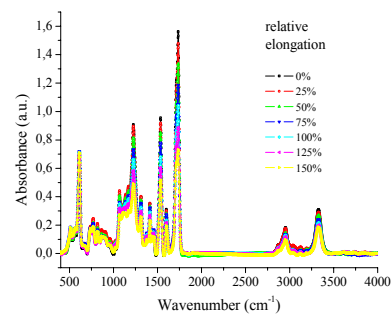
(b)



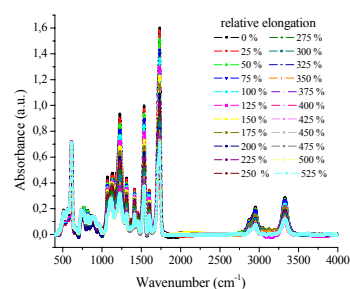
(c)

Fig. 2. The SEM micrographs of PL (a) and PU (b) air-facing surface films (white stick mark is $4\ \mu\text{m}$) and (c) PU transversal section film of PU (white stick mark is $25\ \mu\text{m}$).

In Fig. 3 are presented SLD-IR ordinary spectra of PL (a) and PU (b) films, for different degree of stretching. The relevant differences between ordinary and extraordinary SLD-IR are showed in Fig. 4 for PL (a) and PU (b) films.

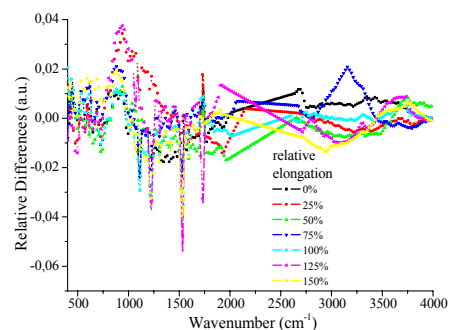


(a)

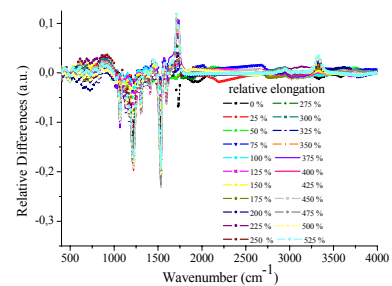


(b)

Fig. 3. SLD-IR ordinary spectra of PL (a) and PU (b) films, for different degree of stretching.



(a)



(b)

Fig. 4. Ordinary and extraordinary SLD-IR differences spectra of PL (a) and PU (b) films, for different degree of stretching.

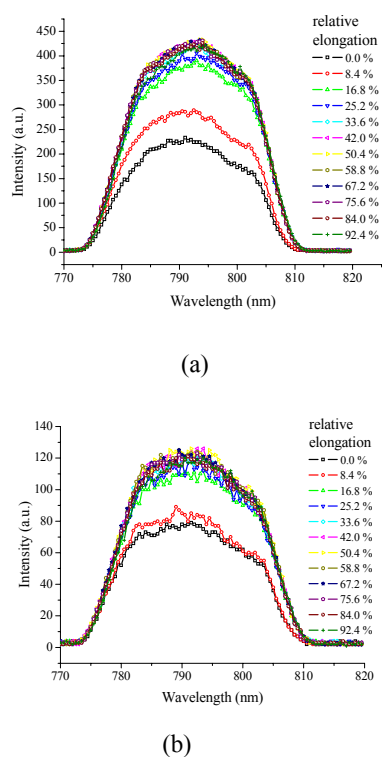


Fig. 5. SLD-UV ordinary (a) respectively extraordinary (b) spectra of PL film, for different degree of stretching (experimental set-up mode 1).

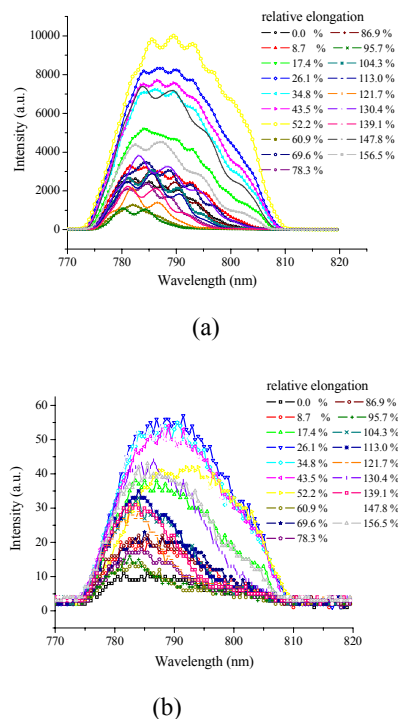


Fig. 6. SLD-UV ordinary (a) respectively extraordinary (b) spectra of PU film, for different degree of stretching (experimental set-up mode 1).

Ordinary and extraordinary SLD-UV spectra of PL and PU are presented in Figs. 5 and 6 respectively, for an experimental set-up when the axis of excitation linear polarized light form with normal weight lead thread 0° -mode 1.

4. Discussion

Detailed discussion about the characteristic band groups are presented in references [10,11].

Important differences between the PL and PU in SLD-IR spectra were noticed within $800\text{--}1800\text{ cm}^{-1}$.

During the stretching there is not observed a shift from N – H bounded to unbounded band; this shows the possibility of instantaneous hydrogen bounds rebuilding.

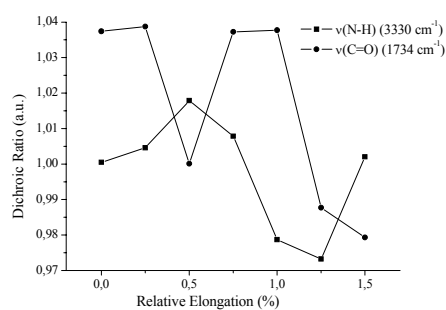
The surface ratio of $(\text{C}=\text{O})_{\text{ester}}/(\text{C}=\text{O})_{\text{urethane}}$ peaks at 1730 cm^{-1} and 1705 cm^{-1} , suggests that the structure of PL is more amorphous as compared with PU due to the lactate segment [11].

When the light polarization is parallel to the long axis, it shall have preferential absorbance both in the N – H stretching region at 3330 cm^{-1} and in the Amide I region at 1698 cm^{-1} (Fig. 4); when the polarization is perpendicular to the long axis, preferential absorbance has the Amide II band corresponding to N-H band (1533 cm^{-1}). This reveals the partially α -helix character of the secondary structure.

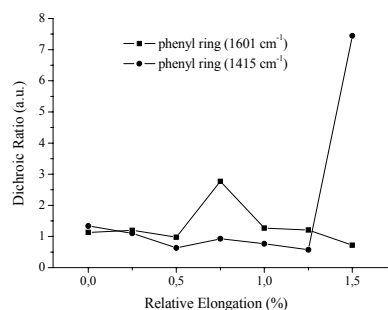
In order to obtain more information it was computed the dichroic ratio, R , for N – H stretching, 3334 cm^{-1} inter-correlated with C = O bound, and phenyl ring bands (Fig. 7 for PL and Fig. 8 for PU).

When the polyurethane is not tensioned, the hydrogen binding under cyclic form prevails. By stretching, some of the hydrogen bindings undo themselves. When the stretching degree of the thin sheets increases, the dichroic ratio measured on N – H bound band after a relative small increases, succeeded by a decreases, the cycle is repeated by increase after stretching more than 125 %. The C = O bound firstly have an opposite behaviour and for a relative elongation of about 100 % decreases sharply. This reveals the dynamics of hydrogen broken bounds rebuilding. The phenomena are similar for the two polymers but while PL is more fragile, the PU can be strain more than 300 % and at this value the C = O (\cdots N – H) bounded urethane become practically linearly with polarized light after that being brooked (Fig. 8a).

Linear decrease of dichroic ratio for phenyl ring starts from 1 (statistically random orientation) and evolves to 0.3 (preferential orientation of phenyl rings dipoles is perpendicular to stretching axis).

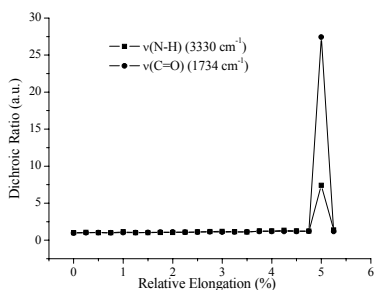


(a)

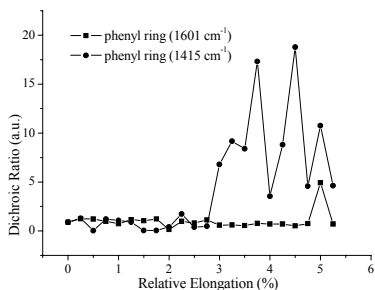


(b)

Fig. 7. Dichroic ratio, R , for $N-H$ stretching, inter-correlated with $C=O$ bound (a), and phenyl ring bands (b) of PL.

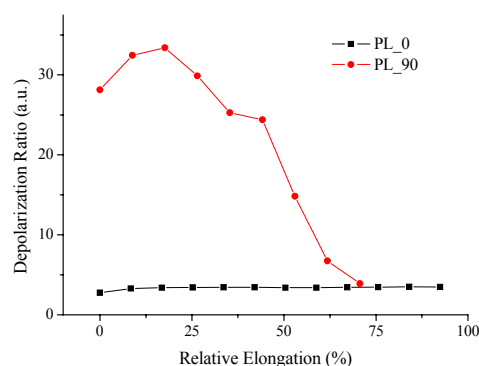


(a)

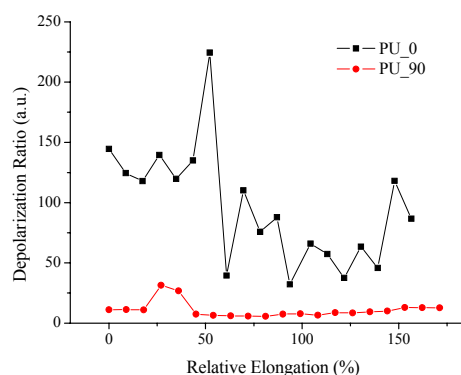


(b)

Fig. 8. Dichroic ratio, R , for $N-H$ stretching, inter-correlated with $C=O$ bound (a), and phenyl ring bands (b) of PU.



(a)



(b)

Fig. 9. Depolarization ratio of PL (a) and PU (b) for different degree of stretching.

After of 50 % relative elongation, the torsion of helix determine the relative reorientation of phenyl rings that is represented in diagram by oscillations of dichroic ratio. When the α -helix structure is formed the angle between phenyl ring and $N-C=O$ plane is around 27 degrees [11].

Less dichroic phenomena were observed for PL spectra (Fig. 4a) comparatively with PU (Fig. 4b). That reveals a very low organization of molecular structure compared with PU, due to the lactate segment.

Inspection of SLD-UV spectra for PL (Fig. 5) and PU (Fig. 6) shows that PU molecules are more packed than PL molecules (depolarization ratio less than 0.006 for PU and less than 0.3 for PL).

Also, while the PL ball packed molecules are destroyed during the stretching process, the PU ball packed molecules suffer a de-folder and re-folder process determined by instantaneous hydrogen bonds broken and rebuilding. That can explain the high mechanical elasticity of PU comparatively with PL.

This experimental results are in good agreement with the *in vacuo* structure of this series of polyurethanes [11].

5. Conclusions

Structural investigations by SLD-IR and SLD-UV reveal the partially α -helix character of the secondary structure due to the hydrogen inter- and intra- bounds chains. The shape of secondary structure of studied polyurethanes depends on urethane group concentration and soft segment structure. A low order secondary structure was observed for PL comparatively with PU, due to the lactate segment. The anisotropy of polyurethane films can be increased by stretching the samples along the casting induced anisotropy direction. Stretching determines the breaking of the hydrogen bonds characteristics to α -helix structure and in the same time the reorientation of the α -helix polymer chains.

References

- [1] P. A. Gunatillake, R. Adhikari, *European Cells and Materials* **5**, 1 (2003).
- [2] H. Shintani, *Biocompatibility and Biostability of Implanted Polyurethane*, *Trends in Biomaterials & Artificial Organs* **14**(2), 17 (2001).
- [3] V. Tura, M. O. Apostu, V. Melnig, C. Ciobanu, B. A. Hagi, *Timisoara Medical Journal* **53**, 127 (2003).
- [4] V. Melnig, M. Apostu, V. Tura, C. Ciobanu, *Journal of Membrane Science*, Article in Press, 10 pg.; Available, 7 July 2005 in Science Direct.
- [5] Y. Osada, T. Nakagawa (Eds.), *Membrane Science and Technology*, Marcel Dekker Inc. (1992).
- [6] J. L. Koenig, *Spectroscopy of Polymers*, American Chemical Society, Washington, (1992).
- [7] B. Gruska, A. Rosler, *Surface and Thin Film Analysis: Principles, Instrumentation, Applications*, Eds. H. Bupert, H. Jenett, Wiley-VCH Verlag GmbH (2002).
- [8] J. D. Ingle Jr., S. R. Crouch, *Spectrochemical Analysis*, Prentice-Hall International, Inc., (1988).
- [9] A. D. Crodd, R. A. Jones, *An Introduction to Practical Infra-Red Spectroscopy*, Butterworth & Co. Ltd., (1969).
- [10] V. Melnig, C. Ciobanu, M. O. Apostu, V. Tura, *Timisoara Medical Journal* **53**, 72 (2003).
- [11] V. Melnig, M. Apostu, V. Tura, C. Ciobanu, *Journal of Membrane Science*, Article in Press, 10 pg.; Available, 7 July 2005 in Science Direct.

*Corresponding author: vmelnig@uaic.ro